NASA TECHNICAL MEMORANDUM

NASA TM X-68261

NASA TM X-68261

APPLICATION OF FINITE DIFFERENCE TECHNIQUES TO NOISE PROPAGATION IN JET ENGINE DUCTS

by Kenneth J. Baumeister
Lewis Research Center
Cleveland, Ohio 44135

TECHNICAL PAPER proposed for presentation at
Winter Annual Meeting of the American Society
of Mechanical Engineers
Detroit, Michigan, November 11-15, 1973

APPLICATION OF FINITE DIFFERENCE TECHNIQUES TO NOISE PROPAGATION IN JET ENGINE DUCTS

by Kenneth J. Baumeister

Lewis Research Center
National Aeronautics and Space Administration
Cleveland, Ohio 44135

E-7551

ABSTRACT

A finite difference formulation is presented for wave propagation in a rectangular two-dimensional duct without steady flow. The difference technique, which should be useful in the study of acoustically treated inlet and exhausts ducts used in turbofan engines, can readily handle acoustical flow field complications such as axial variations in wall impedance and cross section area. In the numerical analysis, the continuous acoustic field is lumped into a series of grid points in which the pressure and velocity at each grid point are separated into real and imaginary terms. An example calculation is also presented for the sound attenuation in a two-dimensional straight soft-walled suppressor.

INTRODUCTION

Because of increasingly stricter environmental noise regulations, noise suppressors are now an integral part of turbojet engine design and other industrial turbomachinery applications. In the particular example of the aircraft industry, turbojet suppressors must be optimized for minimum weight and length to decrease the direct operational cost of the aircraft and to increase the return on investment.

Generally, aircraft suppressors dissipate acoustical energy by viscous action in walls containing absorbing materials. Presently, estimates for the attenuation of acoustic energy (noise) in suppressor ducts are based on the analytical study (refs. 1-7) of acoustic waves propagating into infinitely long straight ducts with uniform impedance (absorbers) along the walls. The analytical techniques, however, are limited to relatively simple geometries.

At the present time, there is a need for more flexible suppressor design techniques which can handle acoustical flow field complications in engine ducts such as axial variations in wall impedance and cross sectional area as would occur in a sonic inlet. To meet the need, the present paper develops a numerical finite difference technique which can be used in the prediction of sound attenuation in turbojet engine ducts as well as other environmental noise abatement problems.

In particular the present paper formulates a solution to the Helmholtz equation with finite wall impedance by a difference technique. The difference solutions bypass the conventional eigenvalue problem with its associated modes which have been considered in earlier works on noise propagation in ducts (refs. 1-7). As a result of the difference formulation, the propagation of noise is treated as a diffusion process analogous to problems in thermodynamics involving heat flow or fluid dynamics involving the transport of vorticity.

Immediately following the mathematical development of the difference technique, example solutions are presented for a comparison between the

finite difference and the analytical results for sound propagation in a one-dimensional hard wall duct and a two-dimensional soft walled duct without steady flow.

SYMBOLS

c	speed of sound
dB	decibels, Eq. (19)
E	acoustic power, Eq. (18)
f	frequency
H	channel height, see Fig. 1
I	acoustic intensity
i	$\sqrt{-1}$
L	length of duct
m	total number of grid rows
n	total number of grid column
P'	pressure fluctuation, P'(x', y', t)
p	dimensionless pressure fluctuation, $p(x, y) = p'/p_A$
p_A	amplitude of pressure fluctuation at duct entrance
t	time
u	dimensionless acoustical particle velocity
x, y	dimension axial coordinate, x'/H, and transverse coordinate, y'/H
Δx, Δy	grid spacing
Z	acoustic impedance
ζ	specific acoustic impedance
η	dimensionless frequency (eq. (4))
θ	specific acoustic resistance
κ	acoustic conductance ratio

λ	wavelength
ρ	density
σ	acoustic susceptance ratio
χ	specific acoustic reactance
ω	circular frequency

Subscripts:

'	prime indicates a dimensional quantity
(1)	real part
(2)	imaginary part

Subscripts:

e	exit condition
i, j	i axial index, j transverse index, see Fig. 2
t	transverse y direction
x	axial position
y	transverse position

GOVERNING EQUATIONS AND BOUNDARY CONDITIONS

The operation of a typical turbojet suppressor using a Helmholtz resonator as a noise absorber is shown schematically in Fig. 1. The noise source shown in Fig. 1 has associated with it some initial pressure profile and some entering acoustic energy flux represented by the symbol I (intensity). The entering acoustic energy is dissipated along the length of the duct by viscous action in the Helmholtz absorbers imbedded in the walls of the duct. The acoustic particle fluid velocities u'_x and u'_y shown in Fig. 1 play an important role in the dissipation process as well as in the transmission of the acoustic energy along the duct. The governing equations

and initial and boundary conditions which describe the transmission and absorption process will now be presented.

WAVE EQUATION

The governing differential equation describing the propagation of acoustical energy in the wave equation. The two dimensional form of the wave equation without steady flow is given by

$$\frac{\partial^2 P'}{\partial x'^2} + \frac{\partial^2 P'}{\partial y'^2} = \frac{1}{c^2} \frac{\partial^2 P'}{\partial t^2} \tag{1}$$

In the above equation, the prime, ', is used to denote a dimensional quantity. These and all other symbols used in this report are defined in the list of symbols. As customary for steady state, the solution is assumed to be of the form

$$P'(x', y', t) = p'(x', y')\, e^{+i\omega t} \tag{2}$$

Substituting Eq. (2) into Eq. (1), and introducing the dimensionless parameters, p, x, y and η yields the classic Helmholtz equation.

$$\frac{\partial^2 p}{\partial x^2} + \frac{\partial^2 p}{\partial y^2} + (2\pi\eta)^2 p = 0 \tag{3}$$

where the dimensionless frequency η is given as

$$\eta = \frac{H}{2\pi} \frac{\omega}{c} = \frac{Hf}{c} = \frac{H}{\lambda} \tag{4}$$

The frequency parameter η represents the ratio of duct height H to acoustic wavelength for the geometry shown in Fig. 1. The dimensionless height y ranges from zero to 1 while the dimensionless length x ranges between zero and L/H.

When using the exponential notation displayed in Eq. (2), the dimensionless pressure p has in general both real and imaginary parts. Thus,

$$p(x, y) = p^{(1)}(x, y) + ip^{(2)}(x, y) \tag{5}$$

Consequently, Eq. (3) can now be broken into its real and imaginary parts by substituting Eq. (5) into Eq. (3),

$$\frac{\partial^2 p^{(1)}}{\partial x^2} + \frac{\partial^2 p^{(1)}}{\partial y^2} + (2\pi\eta)^2 p^{(1)} = 0 \tag{6}$$

$$\frac{\partial^2 p^{(2)}}{\partial x^2} + \frac{\partial^2 p^{(2)}}{\partial y^2} + (2\pi\eta)^2 p^{(2)} = 0 \tag{7}$$

Equations (6) and (7) represent the basic governing equations for noise propagation which will be solved later.

Acoustic Particle Velocity

The boundary conditions in acoustics are generally given in terms of impedances which relate the pressure and velocity fields at the boundary (see schematic insert in fig. 1). For a harmonic solution of the form given by Eq. (2) and in the absence of convective velocities, the dimensionless momentum equations yield the following expressions for the scalar

velocities in terms of pressure gradients:

$$u_x = i\frac{\partial p}{\partial x} \qquad u_y = i\frac{\partial p}{\partial y} \tag{8}$$

where the dimensionless velocities are defined as

$$u_x = \frac{\rho\omega H}{p_A} u'_x \qquad u_y = \frac{\rho\omega H}{p_A} u'_y \tag{9}$$

Impedance Boundary Condition

The specific acoustic impedance ζ_t is defined as

$$\zeta_t = \frac{Z_t}{\rho c} = \frac{p'}{\rho c u'_y} \qquad \text{at } y = 0 \text{ and } 1 \tag{10}$$

where Z_t is the acoustic impedance. Equation (10) can also be expressed in dimensionless form as

$$\zeta_t = -\, i2\pi\eta \frac{p}{\frac{\partial p}{\partial y}} \qquad \text{at } y = 0 \text{ and } 1 \tag{11}$$

It is convenient to express the reciprocal of the impedance ratio in terms of the acoustic conductance ratio κ_t and the acoustic susceptance ratio σ_t, that is,

$$\frac{1}{\zeta_t} \equiv \kappa_t - i\sigma_t \tag{12}$$

where $1/\zeta_t$ is called the acoustic admittance ratio

Finally, substituting Eq. (12) into Eq. (11), and expressing p in terms of its real and imaginary terms yields

$$\frac{\partial p^{(1)}}{\partial y} = -2\pi\eta\left[p^{(1)}\sigma_t - p^{(2)}\kappa_t\right] \qquad \text{at } y = 0 \text{ and } 1 \qquad (13)$$

$$\frac{\partial p^{(2)}}{\partial y} = -2\pi\eta\left[p^{(2)}\sigma_t + p^{(1)}\kappa_t\right] \qquad \text{at } y = 0 \text{ and } 1 \qquad (14)$$

These are the boundary conditions on pressure to be used at the upper and lower surfaces of the duct.

The impedance at the exit plane, x = L/H, leads to a similar expression except an e subscript would be used in place of t in Eqs. (13) and (14) and the pressure gradient would be with respect to the variable x.

Entrance Conditions

For the entrance pressure profile, the assumption used by Rice (ref. 1) of a uniform profile will be used herein. At the present time, there is insufficient information available to improve on this assumption. For a uniform pressure profile, as will be used in the example considered later,

$$p^{(1)}(0, y) = 1 \qquad p^{(2)}(0, y) = 0 \qquad (15)$$

Axial Acoustic Power

The sound power which leaves a duct and reaches the far field is related to the axial intensity. The axial intensity can be expressed in dimensionless form as

$$I = \frac{2\rho c}{p_a^2} I' = \frac{1}{2\pi\eta} \mathrm{Re}\,(p^* u_x) \tag{16}$$

For hard wall duct with a ρc exit impedance, I is identical to 1 for all frequencies and duct lengths.

In terms of the complex representation, the expression for I becomes

$$I = \frac{1}{2\pi\eta}\left[p^{(2)} \frac{\partial p^{(1)}}{\partial x} - p^{(1)} \frac{\partial p^{(2)}}{\partial x}\right] \tag{17}$$

The total dimensionless acoustic power is the integral of the intensity across the test section

$$E_x = \int_0^1 I(x, y)\, dy \tag{18}$$

The minimum value of E_x will occur at the duct exit, $x = L/H$. At this position, the sound attenuation will be a maximum.

By definition, the sound attenuation (the decrease in decibels of the acoustic power from $x = 0$ to x) can be written as

$$\Delta dB = 10 \log_{10} E_x/E_0 \tag{19}$$

Finite Difference Formulation

Instead of a continuous solution for pressure, the pressure will be determined at isolated grid points, as shown in Fig. 2 by means of the finite difference approximations. The governing equations and boundary conditions can be approximated in difference form (ref. 8) by using either a Taylor series expansion, a variational, or an integral formulation. In this acoustic problem, where the gradient is specified along a boundary, the integration method for generating the finite difference approximations is most convenient.

Wave equation. - The wave equation in finite difference form is developed by applying the integration method (ref. 8, p. 168) to the cell marked No. 1 in Fig. 2. The details necessary for the development of the difference equations are given in Ref. 8 as well as many other texts; consequently, only the final results are now presented. The difference form of the $p^{(1)}$ wave equation, Eq. (6), becomes

$$-p^{(1)}_{i-1,\,j} - p^{(1)}_{i+1,\,j} - \left(\frac{\Delta x}{\Delta y}\right)^2 \left[p^{(1)}_{i,\,j-1} + p^{(1)}_{i,\,j+1}\right] + \left[2 + 2\left(\frac{\Delta x}{\Delta y}\right)^2 - (2\pi\eta\ \Delta x)^2\right] p^{(1)}_{i,\,j} = 0 \qquad (20)$$

which is the basic Helmholtz equation in difference form. Using the same procedure, the difference equation for the $p^{(2)}$ component can also be found.

Similarily, the difference equation derived from Eq. (13) which applies in cell No. 2 in Fig. 1 can be expressed as:

$$p^{(1)}_{i,m}\left[1+\left(\frac{\Delta y}{\Delta x}\right)^2+2\pi\eta\,\Delta y\left(\sigma_t\right)_{i,m}-\frac{(2\pi\eta\,\Delta y)^2}{2}\right]-p^{(1)}_{i,m-1}-\frac{1}{2}\left(\frac{\Delta y}{\Delta x}\right)^2 p^{(1)}_{i-1,m}$$

$$-\frac{1}{2}\left(\frac{\Delta y}{\Delta x}\right)^2 p^{(1)}_{i+1,m}-2\pi\eta\,\Delta y\left(k_t\right)_{i,m} p^{(2)}_{i,n}=0 \qquad (21)$$

Similar difference equations exist at the exit cell mark No. 3 and No. 4.

Axial intensity. - In terms of the difference notation, the axial intensity as given by Eq. (17) can be expressed as

$$I_{ij}=\frac{1}{2\pi\eta\,\Delta x}\left[p^{(2)}_{i,j}\left(p^{(1)}_{i,j}-p^{(1)}_{i-1,j}\right)-p^{(1)}_{i,j}\left(p^{(2)}_{i,j}-p^{(2)}_{i-1,j}\right)\right] \qquad (22)$$

The total intensity across the test section, as given by Eq. (18), is written in difference notation as

$$E_i=\left[\frac{1}{2}I_{i,1}+\sum_{j=2}^{m-1}I_{i,j}+\frac{1}{2}I_{i,m}\right]\Delta y \qquad (23)$$

By evaluating E_i at the entrance and exit positions, taking the log of their ratio and multiplying by 10, as indicated in Eq. (19), the maximum sound attenuation for the duct is determined.

We shall now apply the difference equations to the problem of noise attenuation in a duct.

MATRIX SOLUTION

The collection of the various difference equations at each grid point forms a set of simultaneous equations which can be expressed in matrix notation as

$$A * \overline{P} = \overline{F} \tag{24}$$

where A is the coefficient matrix, $\overline{P}$ is the pressure matrix containing the unknown pressures, and $\overline{F}$ the known matrix containing the various initial conditions, where $\overline{A}$, $\overline{P}$, and $\overline{F}$ are complex in general.

The solution to the matrix Eq. (24) yields the values of the real and imaginary pressures $P^{(1)}$ and $P^{(2)}$ at each point. Once these pressures are known, the intensity at any position can be determined from Eq. (22), and the total intensity can be evaluated from Eq. (23). Finally, the sound attenuation in the duct can be found by substituting the values of the total intensity into Eq. (19).

In considering solutions to Eq. (24), it is convenient to express Eq. (24) in terms of all real quantities. To accomplish this, the matrix $\overline{P}$ is written as a column vector in terms of the $p^{(1)}$ and $p^{(2)}$ pressures and subdivided as follows:

$$\left[\begin{array}{c|c} A_1 & -C \\ \hline C & A_1 \end{array}\right] \left[\begin{array}{c} \overline{P}^{(1)} \\ \hline P^{(2)} \end{array}\right] = \left[\begin{array}{c} \overline{F}^{(1)} \\ \hline F^{(2)} \end{array}\right] \tag{25}$$

The A_1 matrix has a form typical of those matrices found in two-dimensional heat conduction problems, while the C matrix represents the coupling that occurs between the $p^{(1)}$ and $p^{(2)}$ pressures through the impedance boundary conditions. The C matrix is a sparse matrix with only one main diagonal term.

The frequency term $(2\pi\eta\Delta x)^2$ in Eq. (20) subtracts from the term which will occupy the main diagonal element of the coefficient matrix; consequently, for sufficiently high frequencies or spacing parameters, the matrix will no longer be positive definite (ref. 8, p. 68). As a result, conventional iteration techniques cannot be used. However, matrices of the form of Eq. (20) can be solved by elimination techniques. In particular, the Gauss elimination technique will be used to find a solution in the example problem which now follows.

Because iteration techniques cannot be used at present, the finite difference technique cannot currently be applied to complicated problems which require a large number of grid points. Iteration technique or more efficient closed form solution will have to be developed to overcome the present grid size limitations.

EXAMPLE CALCULATION

Two example calculations are present in this section so that a comparison between the finite difference solutions and the analytical solutions can be made. First, the simple case of plane waves propagating down a hard wall duct is presented. This case will allow the comparison of the numerical and analytical pressure profiles down the length of the duct. In addition, a rule of thumb on the required grid space is developed. The

second example will compare the numerical and analytical predictions of the attenuation in a soft walled two-dimensional duct.

ONE-DIMENSIONAL HARD WALL DUCT

Numerical and analytical values of the pressure were computed for the special case of a hard wall duct with a ρc exit impedance. Because there is no variation of pressure in the y direction, the two-dimensional grid lattice shown in Fig. 2 can be reduced to a one-dimensional lattice as shown in the upper sketch of Fig. 3. The calculation was made for a hard wall ($Z = \infty$) duct with an L/H of 1 and an inlet plane wave with a dimensionless frequency η equal to 1. The analytical and numerical values of the acoustic pressure profiles along the duct are shown in Fig. 3. As seen in Fig. 3, the agreement between the numerical and analytical results is good.

By a series of numerical calculations, the number of grid points necessary to get pressure profiles, velocities, and intensity accurate to about four percent was found to be

$$n \gtrsim 12\eta\frac{L}{H}$$

If n is less than one half the value given by this equation the accuracy decreases to 10 percent. The accuracy could be further increased by using a four part derivative approximation for the pressure gradient in Eq. (17).

TWO-DIMENSIONAL SOFT WALLED DUCT

As another example of the finite difference formulation, the maximum noise attenuation will now be calculated for a two-dimensional duct as shown in Fig. 2 with L/H of 0.5 and input plane waves with dimensionless frequencies $\eta = Hf/c$ equal to 0.6 and 1. At present, for two-dimensional solutions, the technique is limited to L/H values of 0.5 or less because of matrix size limitations discussed previously.

The numerical results can be compared to the corresponding analytical results found by using the techniques presented by Rice (ref. 1), which is applicable to infinite ducts (no reflected waves). In the numerical formulation of the infinite duct, the duct can be simulated in a finite length by using an impedance value of ρc ($\kappa_e = 1$; $\sigma_e = 0$) at the exit plane of the duct. For plane wave propagating in a hard-wall duct, a ρc exit impedance leads to zero reflected wave which is analogous to an infinitely long duct. This assumed exit condition is discussed in greater detail in the Appendix of this paper.

The first step in determining the maximum attenuation in the duct is to calculate the attenuation at various Z values in the impedance plane. This is shown in Fig. 4 where

$$\zeta = \frac{Z}{\rho c} = \theta + i\chi \tag{26}$$

The sound attenuation values shown in Fig. 4 were obtained by choosing discrete values of θ and χ throughout the θ-χ plane, calculating the appropriate σ and κ from Eq. (12), solving the matrix Eq. (25) by

Gauss elimination for the pressure distribution, and finally calculating the sound attenuation at the duct exit from Eqs. (23) and (19). The results shown in Fig. 4 were obtained by interpolating between the points to obtain smooth contours. The impedance associated with the peak attenuation is called the optimum impedance.

Because of matrix size limitations in the subprogram used to solve Eq. (25), the technique of varying grid size (ref. 9) was used. This is illustrated in Fig. 5 where the grid spacing Δy is decreased toward zero. The attenuation at the optimum point is found by extrapolating the grid size to zero (dotted portion of the curve). As seen in Fig. 5, the extrapolated numerical value is in agreement with the analytical values calculated from the theory presented by Rice in Ref. 1.

This agreement is very encouraging considering the few grid points (maximum of 50) used in obtaining the results. Once new matrix iteration or elimination techniques are developed, the prognosis for obtaining accurate results for complex problems with a minimum of computer storage and running time is excellent.

STEADY FLOW PROBLEM

At present, I am extending the difference technique to the steady flow case. Because of the added Mach number terms in both the wave equation and the slip boundary condition, the coupling matric C in Eq. (25) becomes tridiagonal. However, these complications have not as yet posed any barriers in obtaining the steady flow solutions.

CONCLUDING REMARKS

A finite difference solution for sound propagation in a two-dimensional soft-walled duct for zero Mach number shows favorable comparison with the corresponding exact analytical results. Because the solution matrix for the acoustical flow field is not positive definite, conventional iteration techniques cannot be used to solve the difference equations. Before the finite differences formulation can be applied to more complicated problems which require a large number of grid points, such as the sonic inlet, iteration techniques will have to be developed to overcome present grid size limitations.

The finite difference formulation is flexible and should be a powerful tool in the solution of more realistic studies of inlet and exhaust ducts of turbofan engines. The present formulation allows complete freedom in choosing the inlet pressure profile and the complex impedance along both boundaries. The extension of the present formulation to both uniform flow and shear flow is straight forward.

APPENDIX - EXIT IMPEDANCE ASSUMPTION

The close agreement between the numerical theory and the corresponding analytical results substantiates the utility of the ρc exit impedance assumption made in the previous section of this report. However, the analytical theories (ref. 1 for example) indicate that certain alterations in the numerical exit conditions are required if the numerical theory is to be in exact agreement with the analysis.

The analytical theory for an infinite duct with no reflected waves assumes the solutions to the wave equation are separable and can be expressed in terms of an infinite number of modes. However, the infinite duct with no reflections could be replaced by a finite length of duct L with the exit impedance at L chosen so that no reflections would occur. For no reflections, the analysis indicates that each mode has its own unique exit impedance. Thus, reflections must be occurring at the duct exit in the numerical calculation since choosing an exit impedance equal to ρc can not possibly simulate all the distinct impedance values required for each mode in the analysis.

Fortunately, in many practical problems, most of the higher order modes decay out and the lowest order mode appears at the exit. A comparison to the analytical results indicates that, in general, the exit impedance associated with the lowest order mode is close to ρc. Nevertheless, it is important to establish a general numerical procedure which will converge to the correct answer.

Overlooking round-off and truncation errors in the numerical calculations, the attenuation calculated by the numerical technique will be greater

than that calculated by the exact analytical technique because of reflections which occur at the exit; that is

$$\left.\Delta dB\right)_{\substack{\text{numerical} \\ 0 \le x \le L}} > \left.\Delta dB\right)_{\substack{\text{analytical} \\ 0 \le x \le L}}$$

The reflected energy appears to have been absorbed by the soft walls in the numerical calculation.

Now, consider the case where an additional length of absorbing liner ΔL is added to the original liner, so that the liner now has a length $L + \Delta L$. If ΔL is chosen sufficiently long, the reflected energy at the duct exit $x = L + \Delta L$ will be absorbed before this energy can reach the previous exit position at $x = L$. Therefore, for soft-walled ducts

$$\lim_{\Delta L \to \infty} \left.\Delta dB\right)_{\substack{\text{numerical} \\ 0 \le x \le L}} = \left.\Delta dB\right)_{\substack{\text{analytical} \\ 0 \le x \le L}}$$

Practically, the liner length need only be increased by some minimum length ΔL until the attenuation for the liner length between $x = 0$ and $x = L$ remains constant to a given percentage.

REFERENCES

1. Rice, E. J.: Attenuation of Sound in Softwalled Circular Ducts. AFOSR-UTIAS Symposium on Aerodynamic Noise, Toronto, 20-21, May 1968.

2. Eversman, W.: The Effect of Mach Number on the Tuning of an Acoustic Lining in a Flow Duct. J. Acoust. Soc. Amer. 48, No. 2 (Part I), pp. 425-428, 1970.

3. Lambert, R. F.; and Tack, D. H.: Influence of Shear Flow on Sound Attenuation in a Lined Duct. J. Acoust. Soc. Amer. 38, 655-666 (1965).

4. Pridmore-Brown, D. C.: Sound Propagation in a Fluid Flowing Through an Attenuation Duct. J. Fluid Mechanics 4, 393-406 (1958).

5. Mungur, P.; and Gladwell, G. M. L.: Acoustic Wave Propagation in a Sheared Fluid Contained in a Duct. J. Sound Vib. 9 (1), 28-48 (1969).

6. Savkar, S. D.: Propagation of Sound in Ducts with Shear Flow. Journal of Sound and Vibration 19, 355-372 (1971).

7. Shankar, P. M.: An Acoustic Refraction by Duct Shear Layers. Journal of Fluid Mechanics 47, 81-91 (1971).

8. Varga, Richard S.: Matrix Iteration Analyses, Prentice-Hall, Inc., 1962.

9. Moon, Parry and Spencer, Domina Eberle: Field Theory for Engineers. Van Nostrand, 1961.

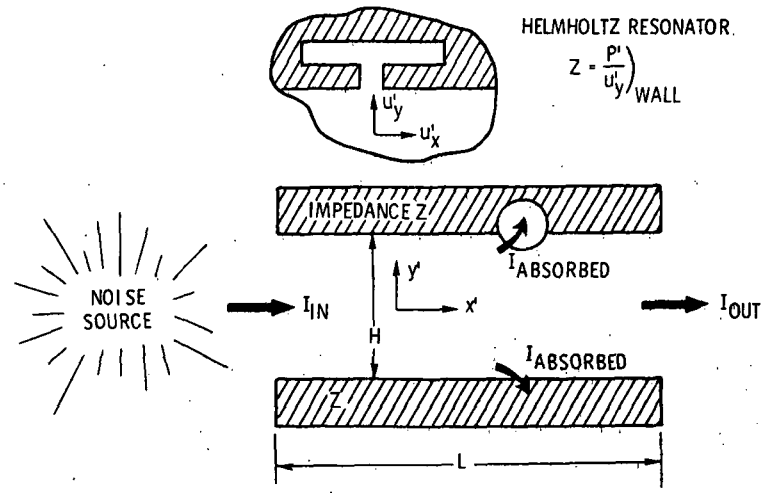

Figure 1. - Schematic of turbojet suppressor duct.

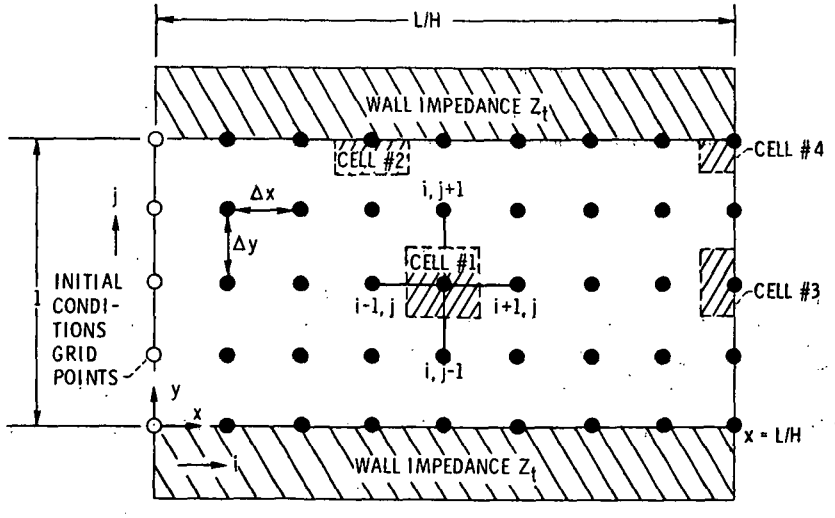

Figure 2. - Coordinate and grid point representation of two dimensional soft walled duct.

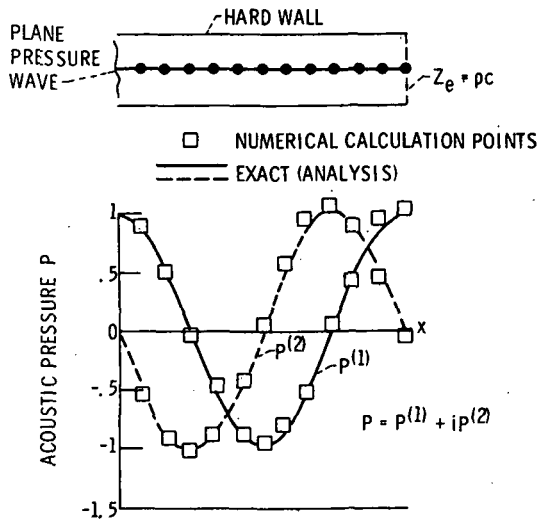

Figure 3. - Analytical and numerical pressure profiles for one dimensional sound propagation with ρc exit impedance for $\eta = 1$ with $n = 12$.

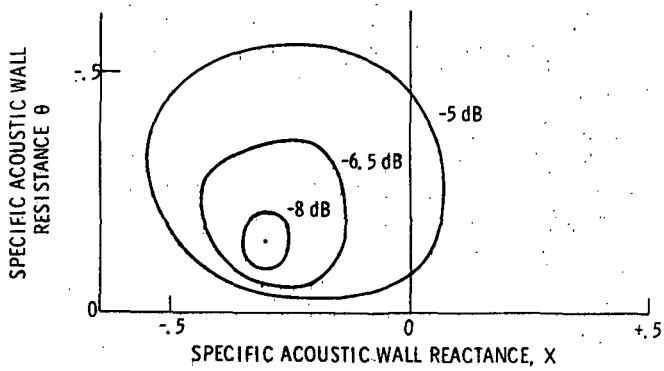

Figure 4. - Sound power attenuation contours for $\eta = 0.6$, $L/H = 0.5$ and $m = 20$, $n = 5$.

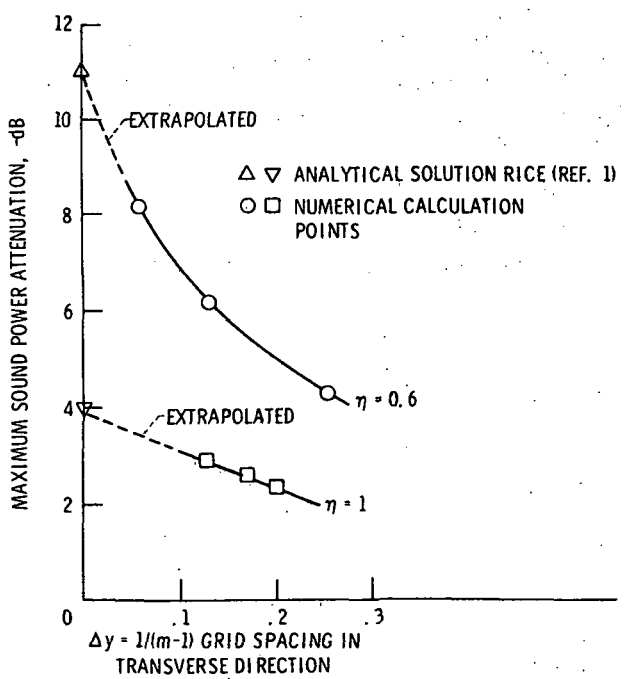

Figure 5. - Effect of spacing on attenuation at optimum impedance in two dimensional duct for $L/H = 0.5$ where $\eta = 0.6$ with $n = 5$ and $\eta = 1$ with $n = 10$.

E-7551